

Ultrafast Coherent EUV at 25-50 nm using the KMLabs XUUS₄TM with the Coherent Astrella[®]



Xiaoshi Zhang, Eric Mountford, Matthew Kirchner, and Henry Kapteyn
KMLabs, Inc., Boulder CO

The Coherent Astrella[®] ultrafast amplifier, combined with the KMLabs XUUS₄TM high-harmonic-generation system, provides stable, high quality, coherent EUV light with photon energy in the range of 25-50 eV, at flux levels enabling a range of scientific applications.



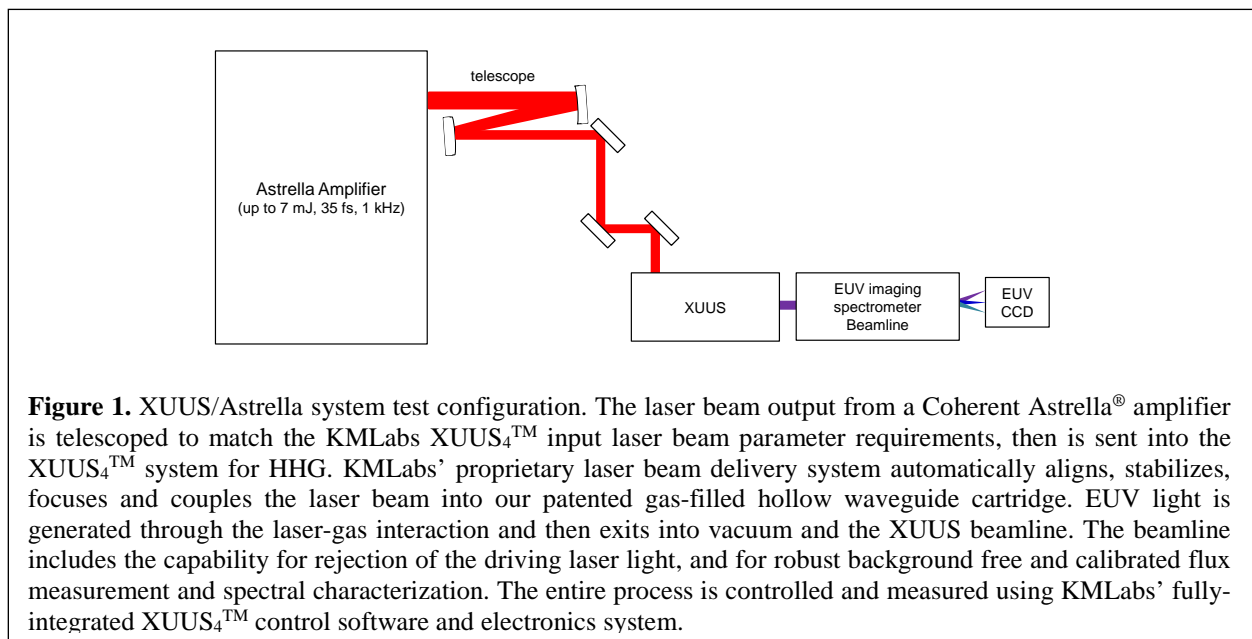
1. Introduction

Just as the invention of the laser has revolutionized science and technology in recent decades, the recent development of tabletop-scale *coherent* laser sources at much shorter wavelengths, EUV and soft X-rays, is likely to have a transformative impact on science and technology applications requiring laser-like performance at these short wavelengths. Coherent EUV is generated using the high-order harmonic generation (HHG) process driven by a high peak-power ultrafast laser.^[1] Applications of HHG light sources include metrology for EUV lithography, spectroscopy, microscopy,^[2] and dynamic studies of molecular,^[3] magnetic,^[4,5] material,^[6] and nano systems.^[7,8] Depending on application requirements, HHG source characteristics can be tailored to obtain attosecond time resolution or energy/spectral resolution as high as 30 meV/0.1 nm,^[9-11] or to enable coherent imaging with spatial resolution as high as 12 nm.^[2]

In the HHG process, an intense femtosecond laser is focused into a gas medium, with the high harmonics generated in the process of field ionization of the gas.^[12] However, optimally implementing an HHG source is not simply a matter of focusing the light into a gas jet or cell: the efficiency of conversion into the EUV depends on multiple parameters, and can vary by orders of magnitude. In early experiments, where the objective was simply to *observe* the generation of high harmonics, this optimization (*phase matching*) was not critical. But as these sources are used in more challenging real-world applications, achieving the highest possible flux becomes increasingly critical for success. In the past, scientists often spent 1-3 years simply in *implementation* of a source. Even then, flux measurements in the EUV are difficult and error-prone enough that the source may be vastly un-optimized and underpowered, thus preventing success in the desired application. A successful implementation of an HHG-based EUV source requires a

comprehensive approach that simplifies flux and spectrum measurement and allows for reliable EUV flux specifications.

KMLabs has developed technology to increase the efficiency of EUV generation through phase-matched conversion in hollow waveguides,^[13-15] and has further optimized the technique in its commercial XUUS₄TM product line.^[16] The three key elements of a workhorse HHG “tabletop x-ray laser” system are: (1) a robust high average power, high repetition-rate femtosecond driving laser; (2) an optimally-implemented, differentially-pumped gas target geometry for high-harmonic generation; and (3) an EUV delivery system engineered to minimize losses and manage thermal loading. This makes it possible to provide a stable, high-quality output beam for applications. KMLabs has supplied their XUUS₄TM system for several years as a fully integrated and specified



system with their DragonTM and WyvernTM ultrafast laser systems; however, the XUUS₄TM and beamline system can be driven by other high-quality ultrafast lasers, such as the Coherent Astrella[®], with appropriate pulse duration, beam quality and stability specs.

2. Test Overview

The configuration used for testing is shown in Figure 1. It consists of the Coherent Astrella[®], the KMLabs XUUS₄TM, and a modularized EUV imaging spectrometer beamline which is one of several of KMLabs’ standard beamline configurations. Here we summarize test results, and show that this configuration makes it possible to produce stable EUV light output in the photon energy range up to ~50 eV (~30 nm) at flux levels that enable a broad set of scientific applications. The entire system, including the laser, the XUUS₄TM, and the beamline occupies single modest-size optical table (~5’x10’).

2.1 Coherent Astrella[®]

The Coherent Astrella[®] amplifier laser system is an industrial-grade one-box ultrafast Ti:sapphire laser amplifier developed and constructed using HALT/HASS techniques for high reliability and dependable performance. It can produce up to 7 mJ per pulse at 800 nm with < 35 fs pulse width at a repetition-rate of 1 kHz (Table 1). All the laser components are in the compact (26 cm x 79 cm x 125 cm) head, including the Vitara[®] oscillator, stretcher, regenerative amplifier with Coherent Revolution[®] Q-switched Nd:YLF laser, and finally a pulse compressor. The Astrella[®] design has been extensively tested for reliability and robust long-term operation.

2.2 KMLabs XUUS₄[™]

The KMLabs XUUS₄[™] is a highly-engineered HHG source and beamline system that allows users to generate coherent EUV light within a day of installation. The XUUS₄[™] HHG source produces EUV with optimal conversion efficiency, while the beamline modules dramatically simplify the delivery of the beam to the experiment with minimum loss, maximum flexibility and wide user customization. This approach lowers the entry barrier into this exciting and new application area of laser science and technology.

KMLabs’s XUUS₄[™] system is built on a single rugged optomechanical platform. It takes a ~0.1-6 mJ energy, 1-100 kHz repetition-rate femtosecond (~<50 fs) laser beam as the input and, depending on the XUUS₄[™] configuration and drive laser parameters, produces a coherent EUV or soft x-ray beam with wavelength that can span from 2 to 50 nm. The KMLabs XUUS₄[™] focuses the pump light into a gas-filled hollow waveguide^[13-15] that keeps the laser focused to high intensity over an extended length, while also providing 100% overlap between the paths of the laser beam and the gas flow. The XUUS₄[™] incorporates a proprietary HHG waveguide cartridge design to implement this patented technology. Optimized differential pumping keeps gas usage to a minimum, allowing even expensive HHG gasses such as Ne, Kr and Xe to be used economically. The EUV generated in the waveguide propagates in a vacuum path produced via efficient differential pumping to avoid re-absorption of the generated light. Compared with a gas jet, gas consumption is orders of magnitude less, and differential pumping allows for optimization of the target pressure while minimizing vacuum pump loading with any gas including Helium (this gas requires a high ~1 atm target pressure that cannot be effectively sustained using other configurations). Different gasses yield HHG spectra that are optimized for different spectral regions, with Xe/Kr ideal for longer wavelengths/lower photon energies, and He best suited for shorter wavelengths (i.e. 13.5 nm).

Since the conversion efficiency of HHG depends strongly on the peak

Parameter	Value
Maximum Pulse energy	7 mJ
Pulse energy used:	
For 30 nm HHG	1.5 mJ
For 13 nm HHG	6 mJ
Center Wavelength	798 nm
Nanosecond Pulse contrast at full power	1959:1 Pre 199:1 Post
Repetition Rate	1 kHz
Beam quality (M²)	1.179 X, 1.194 Y
Pulse Duration (measured by FROG)	33 fs
Beam Size (1/e² Diameter, 2ω₀)	12 mm
Power stability	<0.5% RMS for 8hrs

Table 1: Astrella[®] output pulse parameters as measured for optimum driving of the XUUS₄[™] system.

intensity (i.e. short pulse, tightly focusable beam with $M^2 \sim 1$, minimal ASE), care is also taken in delivering the optimal beam to the focal spot. The XUUS's proprietary laser beam management system maintains both the positional and flux stability of the source over long-term operation. This is achieved thanks to a

computer-assisted automatic laser beam alignment and pointing stabilization system. It also includes a convenient real-time laser beam parameter monitoring and logging system. The result is that the pointing stability of the EUV source exceeds the pointing stability performance of the driving laser—a critical requirement for reliable alignment at EUV wavelengths. The excellent

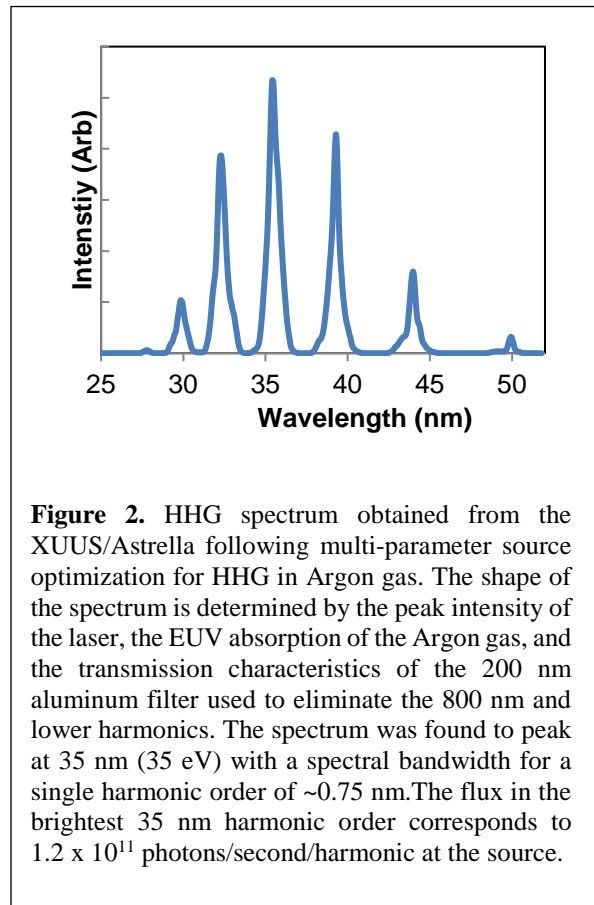


Figure 2. HHG spectrum obtained from the XUUS/Astellra following multi-parameter source optimization for HHG in Argon gas. The shape of the spectrum is determined by the peak intensity of the laser, the EUV absorption of the Argon gas, and the transmission characteristics of the 200 nm aluminum filter used to eliminate the 800 nm and lower harmonics. The spectrum was found to peak at 35 nm (35 eV) with a spectral bandwidth for a single harmonic order of ~ 0.75 nm. The flux in the brightest 35 nm harmonic order corresponds to 1.2×10^{11} photons/second/harmonic at the source.

XUUS ₄ TM Performance using Astrella drive laser	Value
Photon Flux at 35 nm (Argon) --at the source	1.2×10^{11} photons/sec/harmonic
Photon Flux at 13.5 nm (Helium) --at the source	1.5×10^7 photons/sec/harmonic
Spectral range	11 nm to 50 nm (Argon) 25 eV to 112 eV (Helium)
Beam Pointing stability	<10 μ Rad for 1 hour
Power stability	<6.5 % RMS for 1 hour

Table 2: Observed XUUS₄TM Performance when pumped with the Coherent Astrella[®] amplifier.

long-term and short-term stability results in the most stable and usable HHG source implemented to-date. This allows the user to treat the source as a true tabletop “x-ray laser,” rather than as an experiment in itself.

3. Test Results

As a collaborative effort, KMLabs and Coherent conducted HHG measurements at Coherent’s facility in Santa Clara, using a production Astrella[®] laser and XUUS₄TM. After initial characterization of the Astrella[®] output, and implementation of a telescope to adjust the input beam size, the installation of the XUUS₄TM took place over approximately one day.

We evaluated the combined XUUS/Astellra[®] for HHG into two wavelength regions: a) a “near EUV” spectrum generated in Argon gas with the spectrum peaked at ~ 35 nm; and b) a “deep EUV” spectrum generated in Helium gas with spectrum peaked at 13.5 nm. For case a) the optimal pulse energy with the Astrella[®] laser was found to be 1.5 mJ, while for case b) it was 6 mJ. It is

important to note that the full output of the Astrella[®] laser is not needed for EUV generation, so that a good portion of the pulse energy can be reserved for other purposes, such as pumping an OPA for pump-probe experiments.

The measured key EUV parameters are summarized in Table 2. To obtain a quantitative measurement of flux, we used an EUV-sensitive CCD camera cross-referenced to a NIST-traceable EUV photodiode, along with beamline elements with previously-measured throughput. The beamline test configuration and calibration methodology is discussed in more detail in Appendix A.

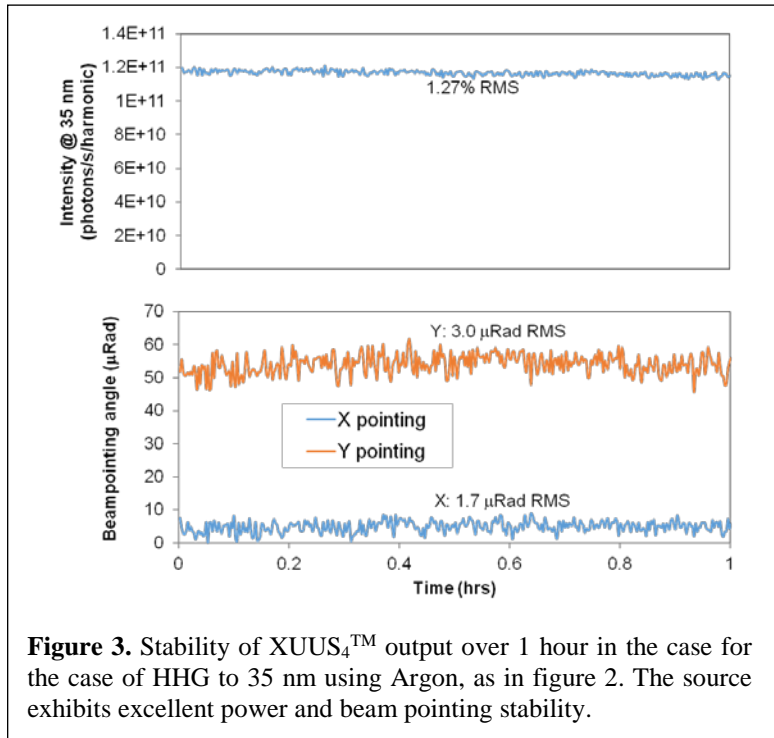


Figure 3. Stability of XUUS₄[™] output over 1 hour in the case for the case of HHG to 35 nm using Argon, as in figure 2. The source exhibits excellent power and beam pointing stability.

The EUV spectrum obtained for case a) and b) are shown in Figure 2 and Figure 4 respectively, while the EUV beam power and pointing stability is shown in Figure 3. The shape of the EUV spectra are the result of several factors, including the peak intensity of the laser at the time during the pulse when the emission is bright and phase-matched, the re-absorption of the longer wavelengths in the Argon gas, and the transmission of the aluminum filters, which were used to reject the fundamental and lower-order harmonics. The spectrum recorded using Ar gas and shown in Figure 2 consists of odd harmonics (17-27th), peaked at the 23rd. The flux measured at the detector corresponds to a flux at the source of 1.2×10^{11} (+/-20%) photons/sec/harmonic for the 23rd harmonic at 35 nm ($h\nu = 35$ eV). The flux measured on the detector was 2.1×10^7 ph/sec, where in this case very thick, high loss Aluminum thin film filters were used to attenuate the beam to avoid detector saturation and ensure an accurate measurement.

In setting-up experiments using EUV light, the discrepancy between the flux at the source and the flux deliverable to an experiment can be very substantial. Optical losses even in a highly-optimized beamline correspond to a throughput typically in the range of 0.1% - 10%. The exact value depends on the throughput of optics used to refocus or select a specific wavelength, as well as the throughput of the thin-film filters used block any visible/NIR light (necessary when using detectors such as CCD's that are sensitive to all wavelengths). *The specifics of the actual experimental application will determine the required throughput of the beam delivery system, and **must** be considered in any calculations of experimental throughput and feasibility.*

Figure 4 shows the spectrum obtained for case b), for high-energy HHG using helium gas. Here, the spectrum is peaked near 13.5 nm, and the flux after optimization was determined to be

$\sim 1.5 \times 10^7$ photons/sec/harmonic, at the source based on a measured flux at the detector of 5.3×10^4 ph/sec. Thus, HHG to 13.5 nm (92 eV) is possible using the Astrella[®]. However, this flux is several orders of magnitude lower than the flux at 35 nm. This mode of operation may be useful for some preliminary spectroscopic studies, and users should expect to use the XUUS₄TM/Astrella[®] setup primarily for HHG up to $h\nu \sim 50$ eV.

4. Summary and Conclusions

The XUUS₄TM system is the culmination of more than 20 years of work by the Kapteyn/Murnane group at the University of Colorado, whose group pioneered 1) the development of ultrafast laser amplifier systems generating 20-30 fs pulses, 2) studies

exploring the basic physics of the high harmonic generation process, and 3) experimental approaches for making use of HHG light in the most demanding applications such as high-fidelity EUV imaging. The test results summarized above provide users of the Coherent Astrella[®] a solid basis for what to expect when using their laser with the KMLabs XUUS₄TM.

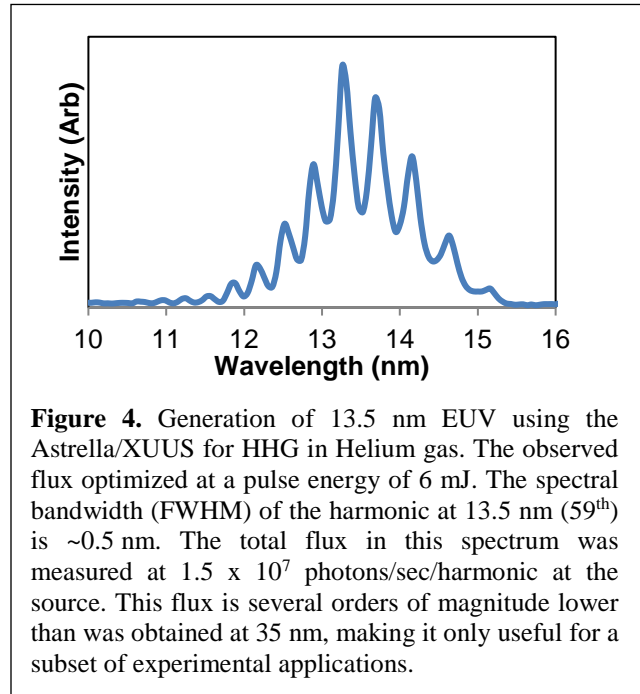


Figure 4. Generation of 13.5 nm EUV using the Astrella/XUUS for HHG in Helium gas. The observed flux optimized at a pulse energy of 6 mJ. The spectral bandwidth (FWHM) of the harmonic at 13.5 nm (59th) is ~ 0.5 nm. The total flux in this spectrum was measured at 1.5×10^7 photons/sec/harmonic at the source. This flux is several orders of magnitude lower than was obtained at 35 nm, making it only useful for a subset of experimental applications.

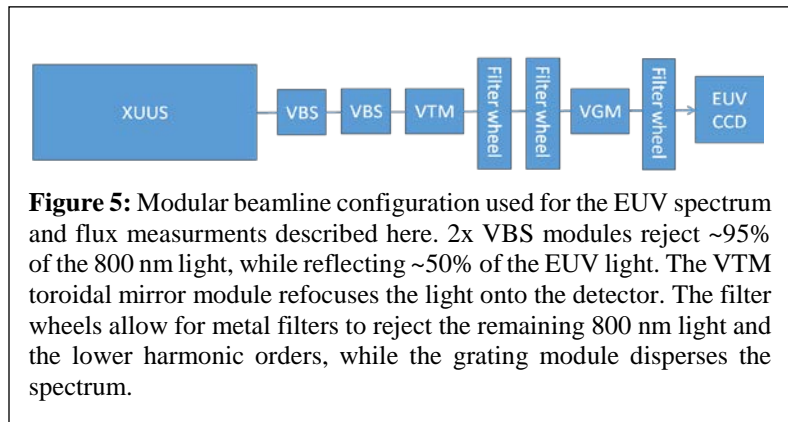
5. References

1. A Rundquist, CG Durfee, 3rd, Z Chang, C Herne, S Backus, MM Murnane, and HC Kapteyn, "Phase-matched generation of coherent soft X-rays," *Science* **280**(5368), 1412-1415 (1998).
2. DF Gardner, M Tanksalvala, ER Shanblatt, X Zhang, BR Galloway, CL Porter, R Karl Jr, C Bevis, DE Adams, HC Kapteyn, MM Murnane, and GF Mancini, "Subwavelength coherent imaging of periodic samples using a 13.5 nm tabletop high-harmonic light source," *Nat Photon* **11**(4), 259-263 (2017). [dx.doi.org/10.1038/nphoton.2017.33](https://doi.org/10.1038/nphoton.2017.33)
3. E Gagnon, P Ranitovic, A Paul, CL Cocke, MM Murnane, HC Kapteyn, and AS Sandhu, "Soft x-ray driven femtosecond molecular dynamics," *Science* **317**(5843), 1374-1378 (2007).
4. D Rudolf, C La-O-Vorakiat, M Battiato, R Adam, JM Shaw, E Turgut, P Maldonado, S Mathias, P Grychtol, HT Nembach, TJ Silva, M Aeschlimann, HC Kapteyn, MM Murnane, CM Schneider, and PM Oppeneer, "Ultrafast magnetization enhancement in metallic multilayers driven by superdiffusive spin current," *Nature Communications* **3**, 1037 (2012). [dx.doi.org/10.1038/ncomms2029](https://doi.org/10.1038/ncomms2029)
5. S Mathias, C La-O-Vorakiat, P Grychtol, P Granitzka, E Turgut, JM Shaw, R Adam, HT Nembach, ME Siemens, S Eich, CM Schneider, TJ Silva, M Aeschlimann, MM Murnane, and HC Kapteyn, "Probing the timescale of the exchange interaction in a ferromagnetic alloy," *Proceedings of the National Academy of Sciences of the United States of America* **109**(13), 4792-4797 (2012). [dx.doi.org/10.1073/pnas.1201371109](https://doi.org/10.1073/pnas.1201371109)
6. C Chen, ZS Tao, A Carr, P Matyba, T Szilvasi, S Emmerich, M Piecuch, M Keller, D Zusin, S Eich, M Rollinger, WJ Youa, S Mathias, U Thumm, M Mavrikakis, M Aeschlimann, PM Oppeneer, H Kapteyn, and M Murnane, "Distinguishing attosecond electron-electron scattering and screening in transition metals," *Proceedings of the National Academy of Sciences of the United States of America* **114**(27), E5300-E5307 (2017). [dx.doi.org/10.1073/pnas.1706466114](https://doi.org/10.1073/pnas.1706466114)

7. KM Hoogeboom-Pot, E Turgut, JN Hernandez-Charpak, JM Shaw, HC Kapteyn, MM Murnane, and D Nardi, "Nondestructive Measurement of the Evolution of Layer-Specific Mechanical Properties in Sub-10 nm Bilayer Films," *Nano Letters* **16**(8), 4773-4778 (2016).
[dx.doi.org/10.1021/acs.nanolett.6b00606](https://doi.org/10.1021/acs.nanolett.6b00606)
8. KM Hoogeboom-Pot, JN Hernandez-Charpak, X Gu, TD Frazer, EH Anderson, W Chao, RW Falcone, R Yang, MM Murnane, HC Kapteyn, and D Nardi, "A new regime of nanoscale thermal transport: Collective diffusion increases dissipation efficiency," *Proceedings of the National Academy of Sciences* **112**, 4846-4851 (2015). [dx.doi.org/10.1073/pnas.1503449112](https://doi.org/10.1073/pnas.1503449112)
9. S Eich, A Stange, AV Carr, J Urbancic, T Popmintchev, M Wiesenmayer, K Jansen, A Ruffing, S Jakobs, T Rohwer, S Hellmann, C Chen, P Matyba, L Kipp, K Rossnagel, M Bauer, MM Murnane, HC Kapteyn, S Mathias, and M Aeschlimann, "Time- and angle-resolved photoemission spectroscopy with optimized high-harmonic pulses using frequency-doubled Ti:Sapphire lasers," *Journal of Electron Spectroscopy and Related Phenomena* **195**, 231-236 (2014). [dx.doi.org/10.1016/j.elspec.2014.04.013](https://doi.org/10.1016/j.elspec.2014.04.013)
10. D Popmintchev, C Hernandez-Garcia, F Dollar, C Mancuso, JA Perez-Hernandez, M-C Chen, A Hankla, X Gao, B Shim, AL Gaeta, M Tarazkar, DA Romanov, RJ Levis, JA Gaffney, M Foord, SB Libby, A Jaron-Becker, A Becker, L Plaja, MM Murnane, HC Kapteyn, and T Popmintchev, "Ultraviolet surprise: Efficient soft x-ray high-harmonic generation in multiply ionized plasmas," *Science* **350**(6265), 1225-1231 (2015).
11. T Popmintchev, M-C Chen, D Popmintchev, P Arpin, S Brown, S Ališauskas, G Andriukaitis, T Balčiunas, OD Mücke, A Pugzlys, A Baltuška, B Shim, SE Schrauth, A Gaeta, C Hernández-García, L Plaja, A Becker, A Jaron-Becker, MM Murnane, and HC Kapteyn, "Bright Coherent Ultrahigh Harmonics in the keV X-ray Regime from Mid-Infrared Femtosecond Lasers," *Science* **336**(6086), 1287-1291 (2012). [dx.doi.org/10.1126/science.1218497](https://doi.org/10.1126/science.1218497)
12. JL Krause, KJ Schafer, and KC Kulander, "HIGH-ORDER HARMONIC-GENERATION FROM ATOMS AND IONS IN THE HIGH-INTENSITY REGIME," *Physical Review Letters* **68**(24), 3535-3538 (1992).
[dx.doi.org/10.1103/PhysRevLett.68.3535](https://doi.org/10.1103/PhysRevLett.68.3535)
13. CG Durfee III, A Rundquist, HC Kapteyn, and MM Murnane, "Guided wave methods and apparatus for nonlinear frequency generation," US Patent #6,151,155 (2000).
14. T Popmintchev, D Popmintchev, MM Murnane, and H Kapteyn, "Method for phase-matched generation of coherent VUV, EUV, and x-ray light using VUV-UV-VIS lasers," US Patent #61/873,794 (Notice of Allowance, 2015).
15. TV Popmintchev, DV Popmintchev, MM Murnane, and HC Kapteyn, "Generation of VUV, EUV, and X-ray Light Using VUV-UV-VIS Lasers," (Google Patents, 2017).
16. KMLabs, "XUUS™ Coherent EUV and Soft X-Ray Source" (2017), retrieved 11/12/2017, <https://kmlabs.com/product/xuus/>.

Appendix A: EUV flux measurement methodology

To accurately measure HHG flux, KMLabs used the beamline configuration as shown in Figure 5. There are many possible pitfalls in the accurate measurement of HHG flux-- primary among them is to block *all* background light from impinging on the detector, both at the fundamental driving laser wavelength of 800 nm, and at harmonic wavelengths that are within the detection



range of the detector, but outside range of wavelengths that are spectrally resolved. KMLabs has developed rigorous procedures that protect against false measurements. In the most rigorous process, the aggregate flux in an HHG beam is measured using a NIST-calibrated photodiode, with the spectrum subsequently dispersed onto a CCD to allow for the flux per harmonic order to be determined.

In this set of measurements, the CCD detector was cross-calibrated at KMLabs with the NIST-calibrated diode, with flux measurements determined using the CCD. Different spectral regions are calibrated using slightly different beamline configurations. For example, in the spectrum of Figure 2, the spectrum from 30-50 nm is isolated using the configuration as outlined in Table 3.

Two filters are used to avoid any 800 nm leakage through small pinholes that are inevitably present in any thin metal filter. Furthermore, since the throughput of these filters decreases with time due to oxidation, a series of three filters is employed in-line. Any two of these is sufficient to block out-of-band radiation, allowing the aggregate transmission of each filter over the spectral region of interest to be accurately measured. The dispersed spectrum is characterized with the CCD, with the flux in a single spectral peak estimated by the integrated counts measured on this detector, previously cross-referenced to the flux measured using a NIST-calibrated diode. A flux at the source can then be backed-out taking into account the beamline efficiency.

Element	Throughput at 35 nm
VBS (2X), IR EUV beam separator module, to absorb 800 nm while reflecting EUV.	~70% each
Aluminum filters (2X), 1000 nm and 200 nm thick, to block 800 nm light as well as lower harmonic orders.	1.8% (1000 nm) 20% (200 nm)
A toroidal refocusing mirror	~70%
Diffraction grating (+1 order)	~16%
Total beamline throughput	0.02%
Total beamline throughput without metal filters	5.5%

Table 3: Beamline configuration and throughput for measurements of near EUV spectrum around 35 nm. Beamline throughput w/o metal filters is also estimated here as many experiments are not IR sensitive such as photoemission microscopy and spectroscopy.

Element	Throughput at 13.5 nm
VBS (2X)	~70% each
Zirconium filters (2X)	18% (200 nm) 16% (200 nm)
Toroidal refocusing mirror	~70%
Diffraction grating (+1 order)	~28%
Total beamline throughput	0.28%
Total beamline throughput without metal filters	10%

For the 13.5 nm spectral measurement, the beamline parameters are given in Table 4.

Table 4: Beamline configuration and throughput for measurements of near EUV spectrum around 13.5 nm. Beamline throughput w/o metal filters is also estimated here as many experiments are not IR sensitive such as photoemission microscopy and spectroscopy.